DOI 10.1002/pmic.200700572 *Proteomics* 2007, *7*, 4278–4291

RESEARCH ARTICLE

Evaluation of protein *N*-glycosylation in 2-DE: Erythropoietin as a study case

Esther Llop[1], Ricardo Gutiérrez Gallego[1, 2], Viviana Belalcazar[1], Gerrit J. Gerwig[3], Johannis P. Kamerling[3], Jordi Segura[1, 2] and José A. Pascual[1, 2]

[1] Pharmacology Research Unit – Bio-analysis group, IMIM, PRBB, Barcelona, Spain
[2] Department of Experimental and Health Sciences, UPF, PRBB, Barcelona, Spain
[3] Bijvoet Center, Department of Bio-Organic Chemistry, Utrecht University, The Netherlands

Received: June 21, 2007
Revised: August 3, 2007
Accepted: August 17, 2007

The structure, function, and physico-chemical properties of many proteins are determined by PTM, being glycosylation the most complex. This study describes how a combination of typical proteomics methods (2-DE) combines with glycomics strategies (HPLC, MALDI-TOF-MS, exo-glycosidases sequencing) to yield comprehensive data about single spot-microheterogeneity, providing meaningful information for the detection of disease markers, pharmaceutical industry, antidoping control, *etc*. Recombinant erythropoietin and its hyperglycosylated analogue darbepoetin-α were chosen as showcases because of their relevance in these fields and the analytical challenge they represent. The combined approach yielded good results in terms of sample complexity (mixture glycoforms), reproducibility, sensitivity (~25 pmoles of glycoprotein/spot), and identification of the underlying protein. Heterogeneity was present in all spots but with a clear tendency; spots proximal to the anode contained the highest amount of tetra-antennary tetrasialylated glycans, whereas the opposite occurred for spots proximal to the cathode with the majority of the structures being undersialylated. Spot microheterogeneity proved a consequence of the multiple glycosylation sites as they contributed directly to the number of possibilities to account for a discrete charge in a single spot. The interest of this combined glycoproteomics method resides in the efficiency for detecting and quantifying subtle dissimilarities originated from altered ratios of identical glycans including *N*-acetyl-lactosamine repeats, acetylation, or antigenic epitopes, that do not significantly contribute to the electrophoretic mobility, but affect the glycan microheterogeneity and the potential underlying related functionality.

Keywords:
2-DE / Erythropoietin / Glycosylation / MALDI-TOF-MS / NESP

Correspondence: Dr. Ricardo Gutiérrez Gallego, Pharmacology Research Unit, Department of Experimental and Health Sciences, Municipal Institute of Medical Research (IMIM), University Pompeu Fabra (UPF), Barcelona Biomedical Research Park (PRBB), C/ Doctor Aiguader, 88. 08003-Barcelona, Spain
E-mail: rgutierrez@imim.es
Fax: +34-93-3160467

Abbreviations: 2-AB, 2-aminobenzamide; **CDG,** congenital disorders of glycosylation; **DHB,** 2,5-dihydroxybenzoic acid; **GU,** glucose units; **LacNAc,** *N*-acetyl-lactosamine; **NESP,** darbepoetin-α; **NP**, normal phase; **PNGase F**, peptide-*N*-glycosidase F; **RAAM,** reagent array analysis method; **rEPO**, recombinant erythropoietin; **rEPO-P**, recombinant erythropoietin from the European Pharmacopoeia Commission; **rEPO-T**, recombinant erythropoietin from Teknika; **WAX**, weak anion exchange

1 Introduction

Proteomics approaches have led to an exponential increase of knowledge of specific proteins involved in a particular cellular process. However, in the routine identification of proteins, the associated PTMs, especially glycosylation, are only partially considered [1]. The biosynthesis of glycans is species, tissue, and cell-type dependent giving rise to so-called microheterogeneity that is exemplified by a large diversity of glycan structures [2]. This is clearly reflected in a 2-DE with the appearance of sets of spots forming characteristic "trains" with similar M_r but different p*I* values [3]. The main factor contributing to the different p*I* values of the glycoforms is the number of negatively charged monosaccharides such as uronic or sialic acids or others such as phosphate or

sulfate groups [4]. The approach presented here combines the typical proteomics techniques with optimized protocols for structural elucidation of glycans. In in-gel peptide-*N*-glycosidase F (PNGase F) digestion, glycan recovery from gel pieces and small-scale purification [1, 5] are combined with several instrumental analyses to achieve maximum sensitivity while minimizing analyte modifications such as loss of labile sialic acid residues during derivatization or fragmentation inside the MALDI ion source [6]. Recombinant human erythropoietin (rEPO) comprises a 165-aa polypeptide chain with one O-linked (Ser-126) and three N-linked (Asn-24, 38, 83) oligosaccharides. Its hyperglycosylated analogue darbepoetin-α (NESP) differs only in 5 aa but has two additional N-linked oligosaccharide chains (Asn-30, 88) [7]. Both are expressed in Chinese hamster ovary (CHO) cells, enriched for the highest sialic acid content [8], and served as model compounds to evaluate the contribution of glycosylation to the migration properties in a 2-DE [9]. Despite the stringent purification criteria rEPO displays seven distinct spots in an IEF gel at p*I* ~4.2 [10] and NESP five at p*I* ~3.3 [7]. Occasionally, IEF is sufficient to correlate a profile to a certain pathology [11]. Still, for most the elucidation of the structural features of the underlying glycoforms will be required. In this context, MALDI-TOF-MS [12] complements IEF allowing the identification of features different from charge (*i.e.*, *O*-acetylation, fucosylation, or *N*-acetyl-lactosamine (LacNAc) repeats). HPLC profiling [13] combined with reagent array analysis methods (RAAM) yields details concerning absolute and relative quantity of a particular glycoform, and the presence of specific structural antigens (*e.g.*, Le^X-fucosylation *versus* core-fucosylation). In conjunction, the glycoproteomic approach described here complements firmly embedded proteomics strategies for the most important PTM. It is expected that this approach will prove its use in different fields among which quality-control of recombinant products [14], detection of recombinant glycoprotein hormone abuse in sports [15], or accurate evaluation of glycosylation-associated pathologies [12].

2 Materials and methods

2.1 Materials

Recombinant human EPO was obtained from the European Pharmacopoeia Commission (rEPO-P) and from Teknika (rEPO-T). NESP was acquired from Amgen. Anti-hEPO mAb (AE7A5) was from R&D Systems. Urea, gelbond film, electrode paper, DTT, and dextran-T70 were from Amersham-Pharmacia. Peptide-N^4-(acetyl-β-glucosaminyl)-asparagine amidase F (PNGase F, EC 3.1.27.5), β-1,4-galactosidase (EC 3.2.1.23), β1-R-*N*-acetylglucosaminidase (EC 3.2.1.97), and α2-3,6,8,9-neuraminidase (EC 3.2.1.18) were purchased from Calbiochem. Carbograph graphitized carbon ultra-clean columns (150 mg) were from Alltech. 2,5-Dihydroxybenzoic acid (DHB), 3,5-dimethoxy-4-hydroxycinnamic acid (SA), and CHCA, iodoacetamide (IAA), BSA, bovine fetuin, and bovine trypsin (EC 3.4.21.4) were from Sigma. 2-Aminobenzamide (2-AB), sodium cyanoborohydride ($NaBH_3CN$), and DMSO were from Fluka. Acrylamide-Bis (97:3, w/w), silver nitrate, and SDS were from Merck; ampholytes Servalyt 2-4 and 4-6 from Serva, and TEMED and ammonium persulfate from BioRad. GELoader Tips were from Eppendorf, Quartz microfibre filters QMA from Whatman, and Supersignal West Femto and biotin-conjugated goat-anti-mouse IgG (H + L) from Pierce. The streptavidin-HRP was from Biospa (SPA). All other chemicals were of highest purity commercially available.

2.2 First dimension (IEF)

IEF was performed as described previously by Lasne *et al.* [15]. In brief, rEPO and NESP samples (sample load ranged from 0.3 ng for chemiluminescence detection to 1–5 μg for 2-DE and silver staining) were focused in a polyacrylamide IEF gel with a pH gradient 2–6 at a constant power of 1 W/cm of the gel length at 8°C until 3600 V·h in a Multiphor-II Electrophoresis system (Amersham-Pharmacia).

2.3 Double immunoblotting and chemilumenescence detection

After focusing, proteins were blotted (0.8 A/cm^2 gel, 30 min) to a PVDF membrane, blocked and incubated with a specific mouse antihuman EPO mAb [15]. The mAb was then reblotted (0.8 mA/cm^2 gel, 10 min) to a second PVDF membrane with 0.7% acetic acid [16]. After blocking, the second PVDF membrane was incubated with biotinylated goat antimouse IgG (H + L) and finally treated with streptavidin-HRP. The primary antibody-secondary antibody-streptavidin HRP complex was detected by addition of peroxidase substrate. Chemiluminescence light was detected using a FUJIFILM-CCD camera LAS-1000.

2.4 2-D-SDS-PAGE and silver staining

After IEF, the strip of interest was excised and placed directly on top of an SDS-PAGE gel. Electrophoresis in a 1 mm, 10%, acrylamide gel was performed using standard protocols for a BioRad Mini-Protean III system (7 cm × 10 cm minigels). Gels were run at 150 V constant voltages in 25 mM Tris/190 mM glycine/0.1% SDS at 4°C. Glycoproteins on gels were visualized by silver staining as described by Shevchenko *et al.* [17].

2.5. In-gel digestion

In-gel digestions followed the method described by Kuster *et al.* [1] with some modifications. Spots were excised from the gel, minced, washed with water, shrunk in ACN for 10 min and dried in a vacuum centrifuge. Then, proteins contained in gel pieces were reduced and alkylated (necessary to com-

pletely de-*N*-glycosylate NESP [18]), by adding 200 μL of 10 mM DTT in phosphate buffer (pH 7.3), left for 30 min at 56°C, and the buffer replaced by a 50 mM IAA solution. After 30 min at room temperature (RT) in the dark with occasional agitation, gel pieces were washed with three cycles of dehydration with ACN, rehydration with phosphate and dried again in a vacuum centrifuge. Deglycosylation was achieved in 50 mM sodium phosphate buffer (pH 7.3) containing PNGase F (1 IU) at 37°C for 24 h. The supernatant containing the released glycans was separated for structural analysis whereas gel pieces were submitted to a tryptic digestion for protein identification.

2.6 Glycan purification

Liberated glycans were desalted with graphitized carbon packed in GELoader tips [19]. The resin was preconditioned in 0.1% TFA in 80% ACN, equilibrated with 50 μL of water, and samples applied. Salts were washed-off with 50 μL of water, while the glycans were eluted with 0.1% TFA in 80% ACN. Carbohydrate fractions were lyophilized and dried at 60°C in a vacuum oven prior to labeling.

2.7 Fluorescence labeling

Oligosaccharide samples were derivatized with 2-AB as described by Bigge *et al.*[20]. A solution of 0.35 M 2-AB in 500 μL DMSO/acetic acid (70:30) containing 1 M $NaCNBH_3$ was prepared. A 10 μL aliquot was added to each sample and the mixture was incubated 2 h at 65°C with intermediate shaking. To eliminate the excess of 2-AB, labeled samples were applied to Whatman QMA paper, allowed to dry and washed with 5 mL of ACN. Carbohydrates were eluted with 1.8 mL of water and lyophilized.

2.8 Exoglycosidase sequencing (RAAM)

N-glycan samples, from solution or in-gel digestions were submitted to either sequential or simultaneous exoglycosidase digestions with α2–3,6,8,9-sialidase, β1-4-galactosidase, β1-R-*N*-acetylglucosaminidase in 50 mM sodium phosphate buffer (pH 6.0) for 16 h at 37°C. Digested samples were filtered over 5 kDa filters, lyophilized, resuspended in 100 μL bidistilled water for HPLC and MALDI-TOF-MS analyses.

2.9 Proteolytic digestion

Erythropoietin samples were digested in 100 mM NH_4HCO_3 (pH 7.8) containing trypsin (ratio enzyme/substrate 1:50) at 37°C for 16 h. In the case of gel pieces, the trypsin containing buffer solution was allowed to rehydrate the gel for 45 min in an ice-bath and then replaced by the same volume of the trypsin-free buffer before incubation.

2.10 Peptide purification

Peptide mixtures from *in situ* digestion of proteins separated by gel electrophoresis or solution digestions were desalted in a GELoader tip packed with 0.5 μL POROS-10 R2 (PerSeptive Biosystem) slurry. The column was conditioned with 10 μL ACN, equilibrated with 10 μL 0.1% TFA, and the acidified sample applied. After washing with 10 μL 0.1% TFA, peptides were eluted with 0.8 μL 0.1% TFA in 80% ACN, containing ~20 g/L CHCA directly onto the MALDI target [21].

2.11 Glycan profiling

The HPLC system used for the profiling consisted of a WATERS 2690 XE module equipped with an in-line degasser, a WATERS temperature control unit (at 30°C) and a 474 scanning fluorescence detector (excitation $\lambda = 330$ nm and emission $\lambda = 420$ nm). The system was controlled *via* a LAC/E interface using WATERS Millennium 32 software.

2.11.1 Weak anion-exchange HPLC

Weak anion-exchange HPLC of N-linked glycans was performed on a VYDAC-301-VHP column (7.5 mm × 50 mm) from VYDAC with the following gradient: solvent A was 50% 500 mM ammonium formate, pH 4.5, 30% water, and 20% ACN; and solvent B was 80% water, 20% ACN. After running 100% B for 5 min, charged *N*-glycans were eluted with a linear gradient of 0–100% A over 40 min at a flow rate of 0.4 mL/min. Initial conditions were reestablished after a 5 min wash-out and equilibrated over the next 15 min. The total run-time was 60 min. The column was calibrated with 2-AB labeled *N*-glycans from bovine fetuin [22].

2.11.2 Normal-phase HPLC

Normal-phase HPLC was carried out on a TSK-gel Amide-80 column (4.6 mm × 250 mm) from TOSOH BIOSEP, using the following gradient conditions: solvent A was 50 mM ammonium formate (pH 4.4), solvent B was 20% solvent A in ACN, and the flow-rate was 0.8 mL/min. Samples were eluted by a linear gradient of 6.5–44% A over 100 min, followed by a linear gradient of 44–100% A over 3 min. Using 100% A the flow-rate was increased to 1 mL/min in 2 min, then the column was eluted with 100% A for 5 min, and subsequently re-equilibrated in 6.5% A before the next sample injection. The system was calibrated in glucose units (GU) using a 2-AB-labeled dextran hydrolysate. The total run-time was 140 min [23].

2.12 MALDI-TOF-MS

Samples (proteins, peptides, or carbohydrates) were dissolved in water, mixed with the corresponding matrix solution, <1 μL of these preparations applied to the MALDI target, and allowed to dry at RT. A solution of SA (10 mg/mL) in ACN/water/TFA

(50:50:0.1 by vol.) was chosen for protein analyses, a solution of CHCA (20 mg/mL) in ACN/water/TFA (70:30:0.1 by vol.) for peptide analyses, and a solution of DHB (10 mg/mL) in ACN/water (50:50 v/v) for *N*-glycan analyses. Experiments were carried out on a Voyager-DE™ STR Biospectrometry workstation (Applied Biosystems), equipped with a N_2 laser (337 nm). Samples were measured both in the linear providing information on the total number of different structures and in the reflectron mode for identification of molecular formulas based on precise mass measurements. External calibrations of the spectrometer were performed with of 2-AB-labeled glucose oligomers in positive ion-mode and 2-AB-derivatized fetuin *N*-glycans in negative mode. For peptides, the Sequazyme™ Peptide Mass Standards Kit (PerSeptive Biosystems) was used to calibrate. Recorded data were processed with Data Explorer™ Software (Applied Biosystems).

3 Results

The overall strategy developed for assessing the glycosylation contained in glycoforms that share a particular p*I* (Fig. 1) was tested using rEPO and NESP as model glycoproteins. First, the total *N*-glycan analysis served to identify and quantify all structures present. Reduction and alkylation was necessary prior to de-*N*-glycosylation of NESP due to the enzyme inaccesibility to Asn-30 under native conditions [24]. Weak anion exchange (WAX) chromatograms of rEPO and NESP (Fig. 2) showed profiles with larger heterogeneity than fetuin [22]. Although the respective profiles were significantly different, both rEPO-P and NESP displayed the absence of neutral glycans, whereas tri- and tetracharged glycans dominated. The main differences resided in the smaller structures; NESP did not contain monocharged structures and only low amounts of dicharged glycans in comparison with rEPO-P. The selective enrichment for high sialic acid content of these pharmaceuticals became evident from a comparison with the profile of nonenriched rEPO (rEPO-T). Neutral, mono-, and dicharged *N*-glycans dominated, low amounts of tricharged structures were present, and tetracharged *N*-glycans were nearly absent (Fig. 2). Following desialylation, WAX profiles showed only neutral structures evidencing the absence of charged groups other than sialic acids. NP-HPLC profiles of the total *N*-glycan pool (Fig. 3) showed that both rEPO's and NESP have GU values comprised between 8 and 14, indicating the presence of predominantly tri- and tetra-antennary complex-type *N*-glycans. GU values higher than 11 potentially indicate the presence of LacNAc repeating units [25].

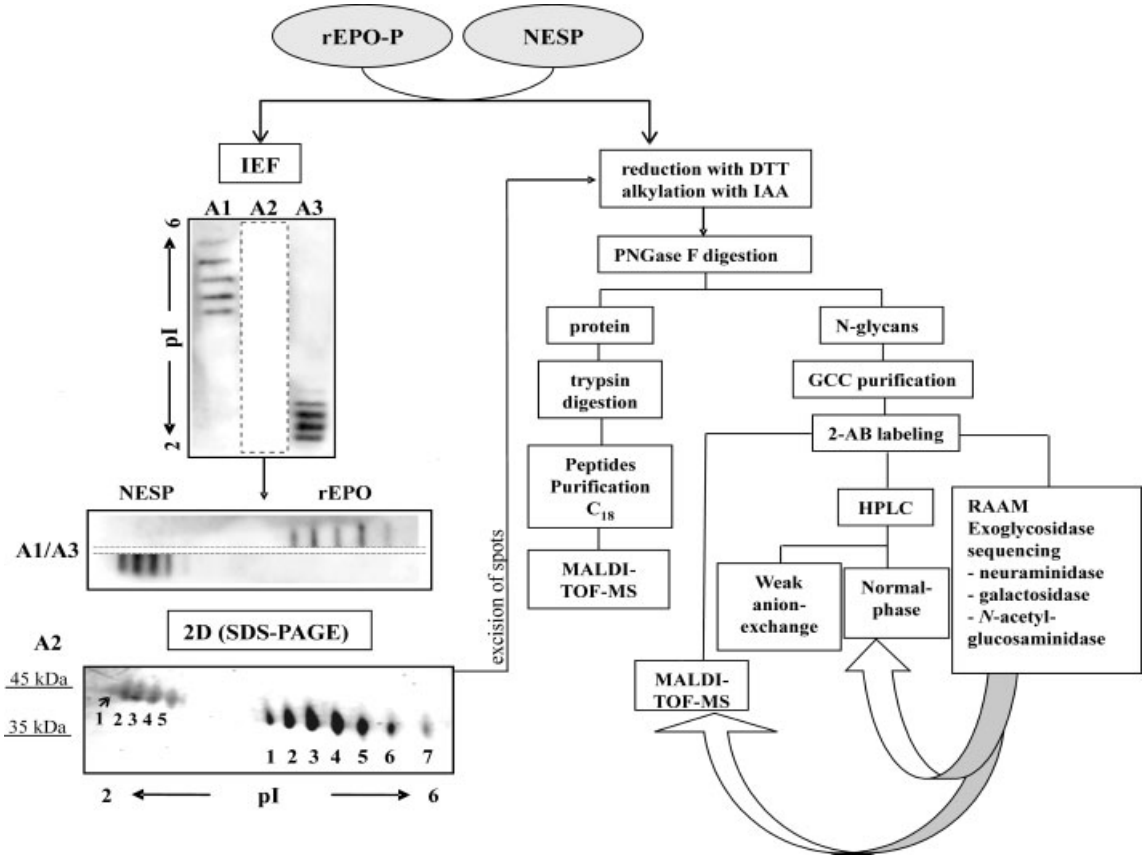

Figure 1. Strategy for analysis of glycoproteins separated in 2-DE. A1 represents rEPO-P, A2 a mixture of rEPO-P and NESP, and A3 represents NESP. The IEF strip of A2 was used for the separation in the second dimension.

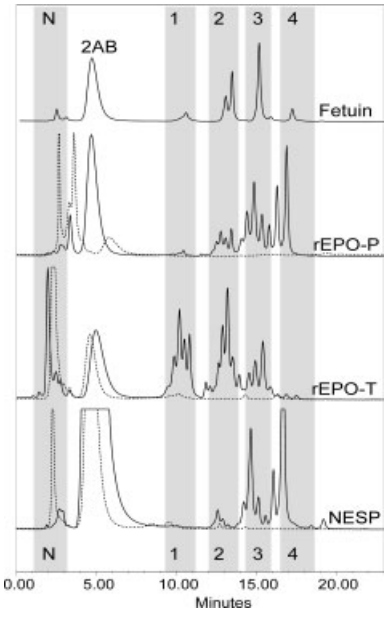

Figure 2. WAX-HPLC profiles of 2-AB-labeled *N*-glycans from fetuin (upper panel, used as standard), rEPO-P (second panel), rEPO-T (thirt panel), and NESP (lower panel). The regions corresponding to neutral (N), mono- di-, tri-, and tetra-sialylated glycans (1, 2, 3, 4) are indicated with grey boxes. 2-AB indicates the excess of reagent. Charge profiles correspond to the original mixture (solid line) and after desialylation (dotted line). The peaks observed in the charged area after desialylation were attributed to incomplete digestion.

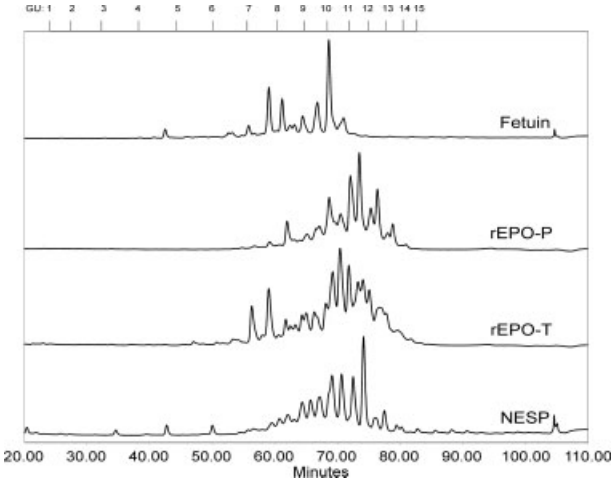

Figure 3. Normal-phase HPLC profiles of 2-AB-labeled *N*-glycans from fetuin (upper panel, used as standard), rEPO-P (second panel), rEPO-T (third panel), and NESP (lower panel). Profiles are standardized against a dextran hydrolysate (GU).

The profiles of rEPO-P and NESP showed peaks in the same GU interval, with main differences in the peak intensity, but it could not be inferred whether these dissimilarities were due to structural differences or whether they originated

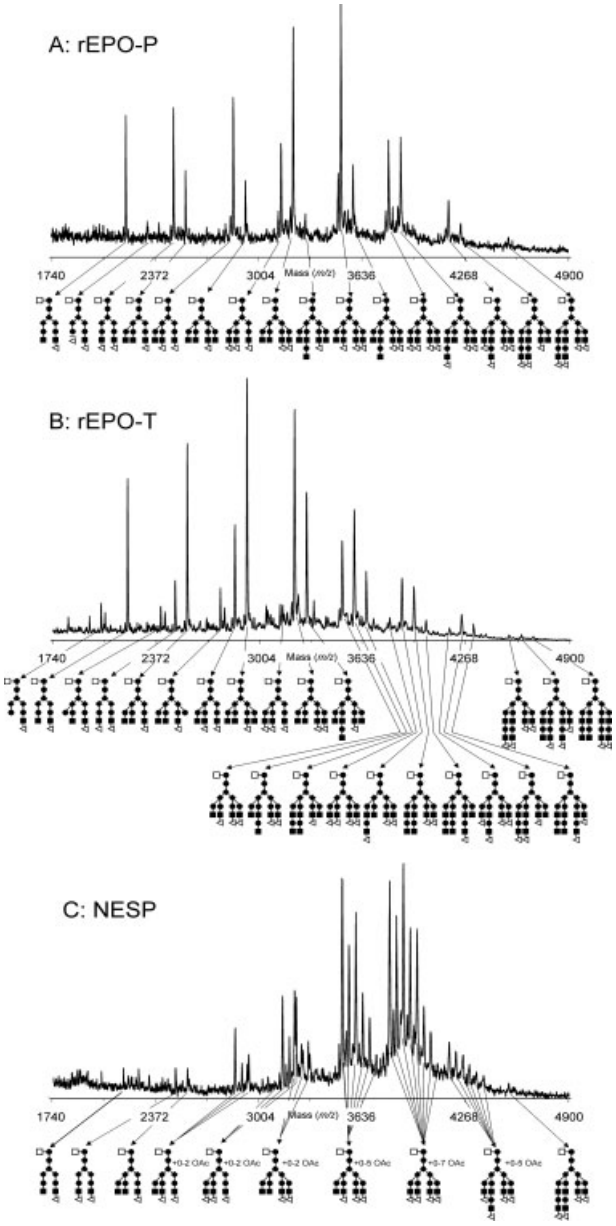

Figure 4. Negative-ion MALDI mass spectra of 2-AB-labeled glycans from recombinant erythropoietins; (A) rEPO-P; (B) rEPO-T; (C) NESP. Structures indicate all possible isomers. Short-hand notation: (□) fucose, (●) *N*-acetylglucosamine, (◆) mannose, (■) galactose, (△) sialic acid. *n*OAc: *O*-acetylated sialic acids residues (where *n* = 0–7 indicate the number of substituents in a single *N*-glycan).

from altered ratios of identical glycans. Further structural information was obtained from MALDI-TOF-MS analyses of the 2-AB-labeled structures. The aromatic moiety, introduced to enable HPLC with fluorescence detection (FLD), enhances significantly the signal intensity [24]. Mass spectrometric profiles of recombinant preparations (Figs. 4A–C) displayed 16–25 different mass values. Structural assignments are based on NMR studies by Hokke *et al.* [26], but must be con-

sidered as representative of all known isomers. The majority of the structures identified in the rEPOs were tetra-antennary complex-type *N*-glycans containing upto four sialic acids, and all were fucosylated. Furthermore, a substantial percentage of these structures contained upto two LacNAc repeats. The comparison of the rEPO-P and rEPO-T spectra corroborated the findings from WAX analyses on the selective enrichment of the pharmaceutical preparation; overall showing a lower degree of end-capping sialic acid residues on identical structures in the latter. When the spectra of the rEPOs were compared to NESP, the latter demonstrated even better the purification of the pharmaceuticals for the highest possible sialic acid content from the nearly complete absence of both neutral and biantennary type structures. From the peak intensities in the mass spectrum it could be deduced that the most abundant glycans corresponded to tetra-antennary, tetrasialylated structures. Furthermore, from the mass values also the presence of LacNAc repeats could be confirmed. The NESP profile differed substantially from that of rEPO-P, even though both are produced in CHO cells. Different degrees of *O*-acetylation were observed by MS (Fig. 4C), evidenced by the cluster of peaks separated by 42 Da [27]. This modification is not easily picked-up by other techniques included in glycoproteomics such as IEF, SDS-PAGE, or HPLC. The occurrence of upto seven *O*-acetyl substituents in a maximum of four sialic acids implies the existence of multiple *O*-acetylation of a single residue. This observation corroborated our results from sialic acid analysis (not shown) in which NESP showed ~6.4% mono-*O*-acetylated species (Neu5,9Ac_2) as well as ~1.2% of di-*O*-acetylated (Neu5, 7, 9Ac_3) molecules. This phenomenon was not so evident in rEPO in which the mono-*O*-acetylated residue (Neu5,9Ac_2) accounted for ~1.3%. Reagent array analyses with an α-2,R-sialidase, a β-1,4-galactosidase, and a β-1,R-*N*-acetylglucosaminidase (Fig. 5) corroborated initial findings. Full digestion yielded the core-fucosylated pentasaccharide (lower panel of Figs. 5A–C) for all samples, and indicated the absence of Lewis-type epitopes. Once all structural heterogeneity was eliminated also the presence of the non-fucosylated core structure was evidenced, albeit with a very low peak intensity. From these data and the corresponding mass spectra (Fig. 6), the sequential dissection of the structural elements did permit the detailed analysis of each mixture, and also accurate quantification of the type of antennae and LacNAc repetitions. NESP showed around 1.3% of biantennae whereas in rEPO this value was ~14%. LacNAc repeats were also more abundant in rEPO (~33%) than in NESP (~13.6%). As rEPO-P and rEPO-T displayed identical structures (with only differences in degree of sialylation), further data (*vide infra*) are described for rEPO-P only.

3.1 Gel-separated glycoforms

Three samples containing 0.3 ng rEPO-P (Fig. 1-A1), 0.3 ng NESP (Fig. 1-A3) and 5 μg rEPO-P plus 5 μg NESP, respectively (Fig. 1-A2), were separated in the first dimension. Fol-

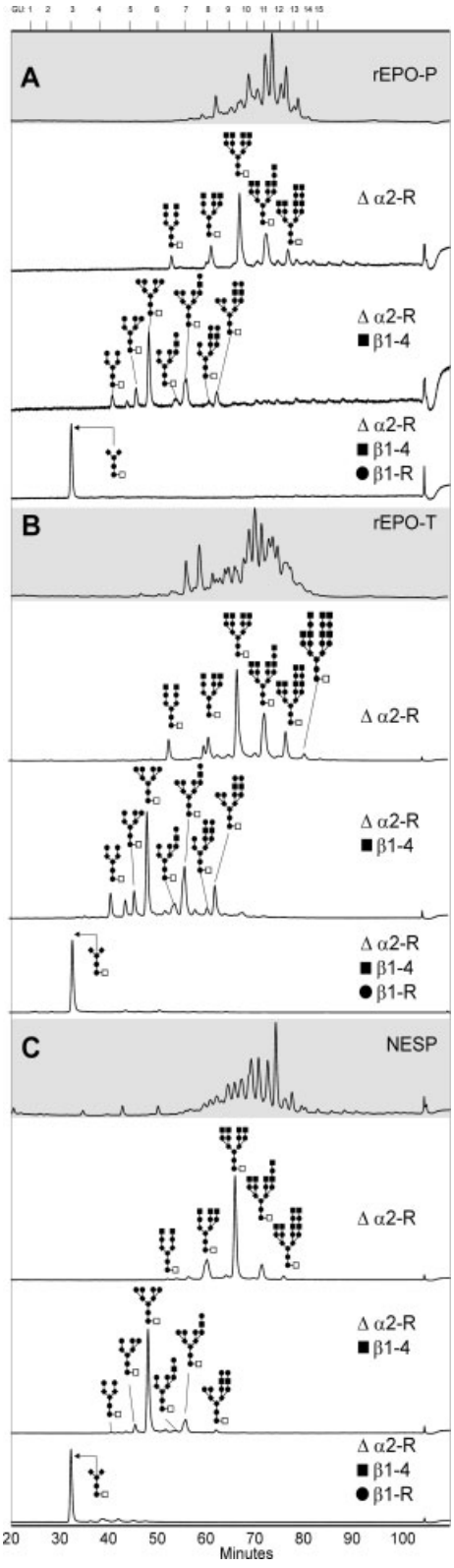

Figure 5. Normal-phase HPLC profiles of 2-AB-labeled glycans from recombinant erythropoietins before (in gray boxes) and after RAAM. (A) rEPO-P; (B) rEPO-T; (C) NESP. △α2-R: sialidase; ■β1-4: galactosidase; ●β1-R: *N*-acetyl glucosaminidase.

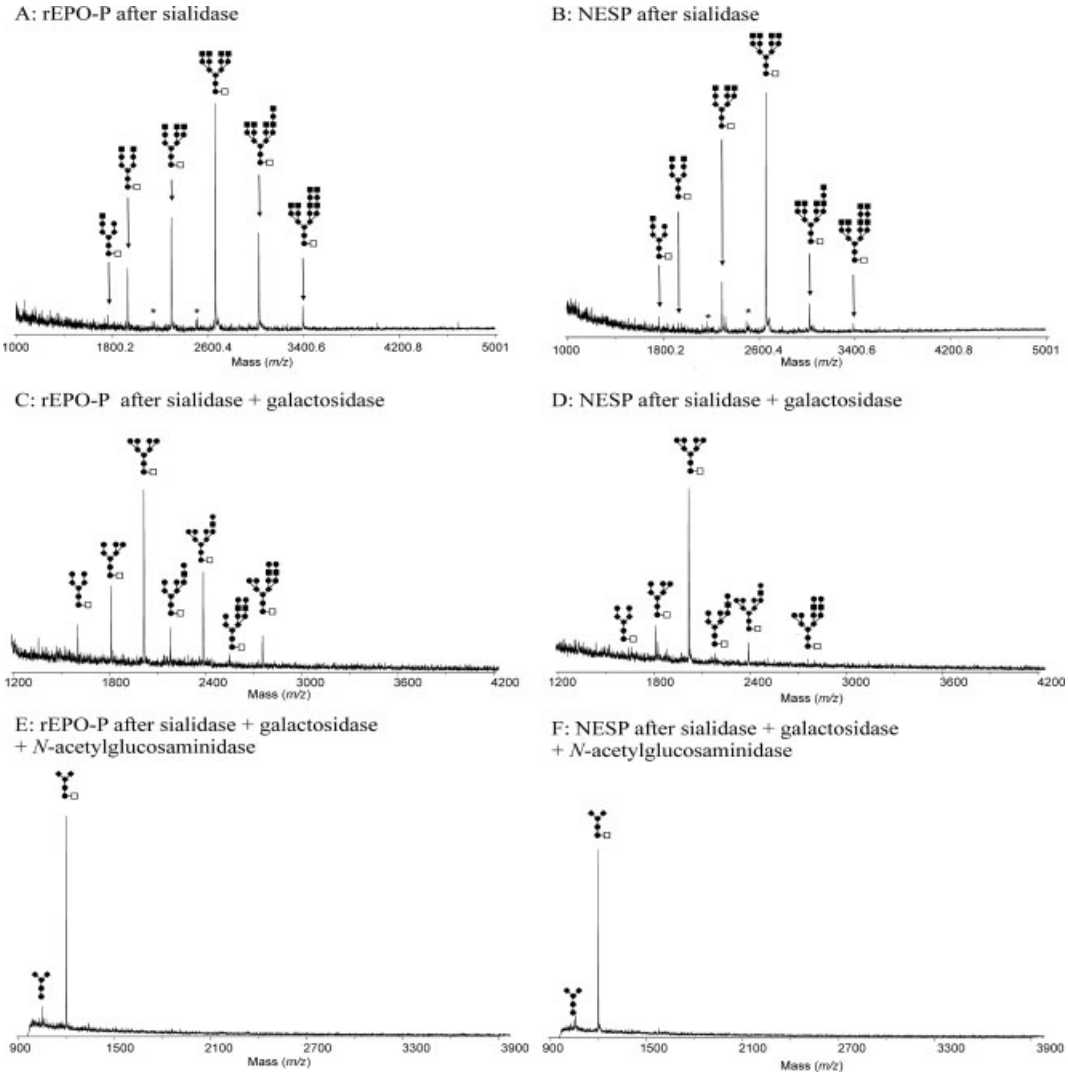

Figure 6. Positive-ion MALDI mass spectra (reflectron mode) of rEPO-P and NESP after exoglycosidase digestions (RAAM). The series corresponding to rEPO-P are on the left (panels A, C, and E). The series corresponding to NESP are on the right (panels B, D, and F). * *m*/*z* of the nonfucosylated structures.

lowing separation the three lanes were excised. The lanes containing either rEPO-P or NESP were processed employing the double-blotting method [16] to identify the corresponding spot in the 2-DE. This was obtained from the third lane (A2), that following excision from the IEF gel was placed directly on top of a 10% SDS gel, separated in the second dimension, and detected through conventional silver staining. The experimental design proved reproducible both in terms of spot-number, spot-intensity, and relative position within the gel. As foreseen for the two molecules, rEPO-P migrated to a M_r of ~35 kDa whereas NESP migrated to a M_r of ~45 kDa, according to their hydrodynamic volume [18, 28]. The influence of sialic acid residues to the separation in both dimensions is evident as it is the only factor contributing to the distinct p*I* values [29] between two adjacent IEF spots that also migrate to different M_r values. In the 2-DE spots were numbered according to their acidity; *i.e.*, rEPO-1 to rEPO-7 and NESP-1 to NESP-5 correspond to increasing p*I* (lower acidity) with increasing number. Following separation and silver-staining, spots were excised, reduced, alkylated, and digested with PNGase F. To ensure that the oligosaccharides originated from rEPO or NESP, and that the observed positional differences of two adjacent spots in the 2-DE gel was not due to other PTM modification, de-*N*-glycosylated spots were digested with trypsin and identified by MALDI-TOF mass mapping (not shown). Released *N*-glycans were purified, labeled with 2-AB and analyzed as described.

As the amount of material contained in each spot is not equivalent, the different WAX profiles were normalized to the highest peak observed, in order allow comparative analysis. Going from rEPO-1 to -7 (Fig. 7A), a progressive decrease in tetra-charged structures with increasing spot number was

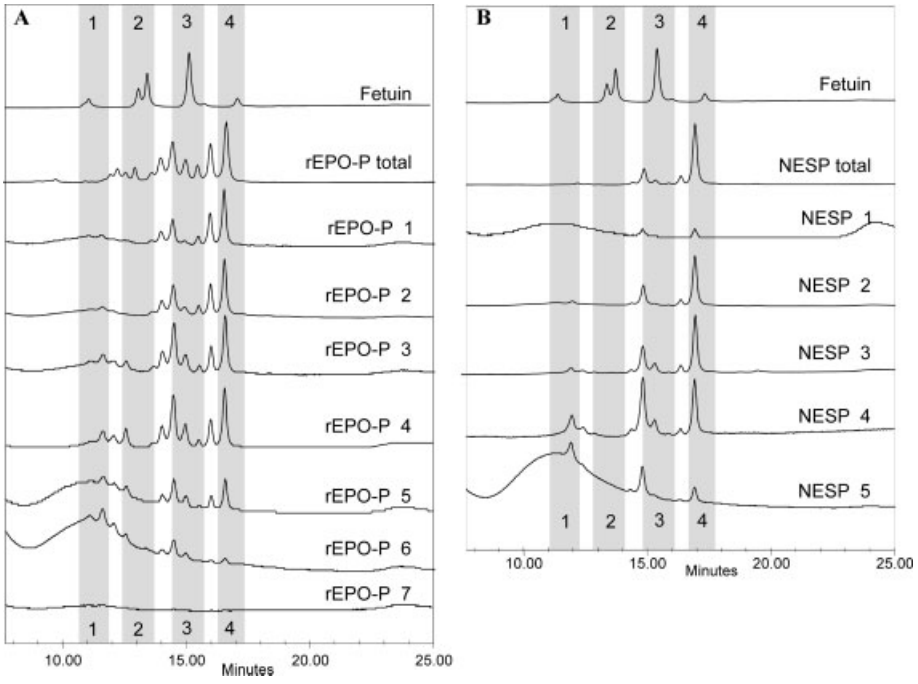

Figure 7. WAX-HPLC profiles of 2-AB-labeled *N*-glycans released from single spots in the 2-DE [rEPO-1 to rEPO-7 (A), and NESP-1 to NESP-5 (B)], indicate the profiles from different spots and are compared with the total *N*-glycan pool (total) and fetuin (upper panel). Number 1 corresponds to the most acid IEF spot whereas number 5 (NESP) and number 7 (rEPO) indicate the most basic IEF spot. The numbers correspond to the mono-, di-, tri-, and tetrasialylated *N*-glycans (1, 2, 3, 4) from fetuin.

accompanied by a progressive increase in dicharged entities. Even though the net difference between the two outer-most spots were evident at first sight, the difference between two adjacent spots was much harder to observe. The WAX profiles were divided into five sections according to the neutral, di-, tri-, and tetracharged structures of bovine fetuin. As before (Fig. 2), no neutral structures were observed which is in agreement with the purification protocols and confirms that sample handling upto this point did not result in significant loss of sialic acid residues. In rEPO-1 the highest peak corresponded to the tetracharged species but its area was equivalent to that of the sum of the peaks belonging to the tricharged structures. The amount of material in the dicharged region was almost negligible. The latter increased gradually, when moving from rEPO-1 to rEPO-4 whereas the peaks corresponding to the tricharged material appeared to remain unaffected and the peak corresponding to the tetracharged species did no longer predominate. In rEPO-5, peaks in di-, tri-, and tetracharged regions appeared equivalent. Finally, in rEPO-6 the amount of tetracharged structures was almost negligible and the dicharged structures were most abundant. For NESP (Fig. 7B) a similar trend was observed; the normalized WAX profiles showed very clear tendencies toward less-charged glycans with increasing p*I* of the spot-number.

Samples were subsequently analyzed by normal-phase HPLC (Fig. 8) giving similar results as obtained with WAX, *i.e.*, predominance of longer retention time for the more acidic spots indicating the presence of both, larger and/or more charged structures as opposed to shorter retention times for the least acid spots. The profiles obtained for three consecutive repetitions after 2-DE separation, glycan release and labeling were nearly identical proving the reproducibility of the approach. When the normal phase profiles of the individual spots were compared, only subtle differences could be observed in these chromatograms because separation is not only according to the charge content. An example of this trend is indicated in Fig. 8B with the peaks that were tentatively assigned to core-fucosylated tetra-antennary complex-type glycans bearing three or four end-capping sialic acid residues. A clear inversion of the peak-ratio can be seen when going from NESP-1 to NESP-5. For rEPO (Fig. 8A), this flip was also observed for the same glycans, albeit that the larger structural heterogeneity in this product rendered a less pronounced phenomenon. Subsequently, all fractions were digested with sialidase and profiled again (Fig. 9). The corresponding normal-phase HPLC profiles displayed nearly identical chromatograms (ratio between different structures). Moreover, the presence of smaller structures (*i.e.*, biantennary complex-type *N*-glycans) in the less charged fractions was also highlighted after the sialidase digestion. Overall, these results confirmed that the separation in the IEF procedure was solely due to the differential content of sialic acid residues.

Finally, to assign the structures from individual spots, and corroborate HPLC results, MALDI-TOF-MS were carried out. All mass spectra (for rEPO in Fig. 10A; for NESP in Fig. 10B) were processed identically to facilitate a quantitative evaluation. The tendency for both is similar as in the chromatographic profiles, *i.e.*, larger structures containing a higher number of sialic acids accompany increasing acidity and reinforced the observation on the contribution of sialic acid residues to the IEF separation.

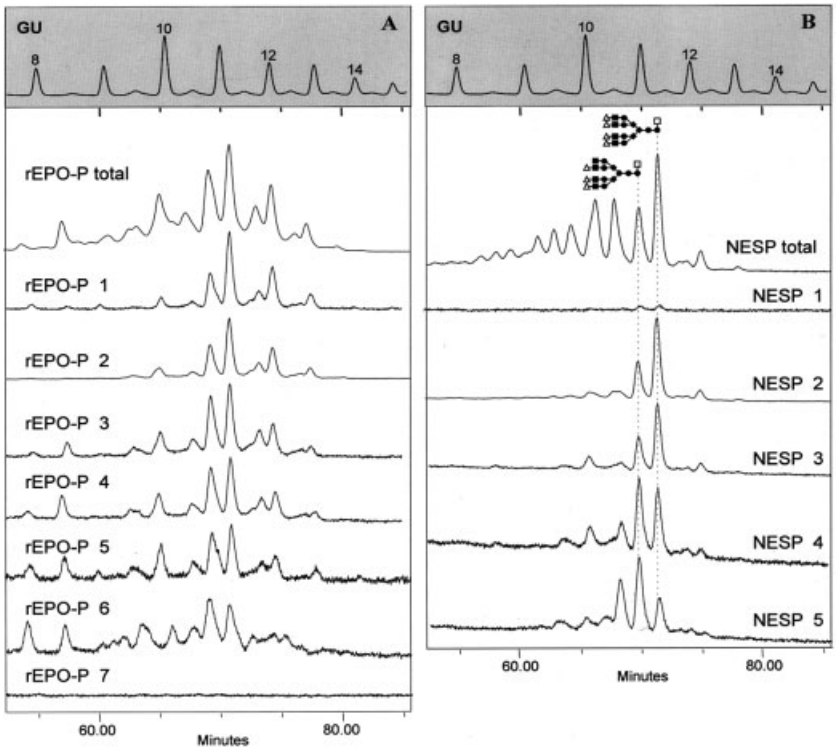

Figure 8. Normal-phase HPLC profiles of 2-AB-labeled glycans from 2-DE spots. (A) rEPO-P (1 for acidic, to 7 for basic spot). rEPO-7 was not detected in this analysis but could be observed in the MS. (B) NESP (1 for acidic, to 5 for basic). Profiles are standardized against dextran hydrolysate (GU) (upper panel in gray).

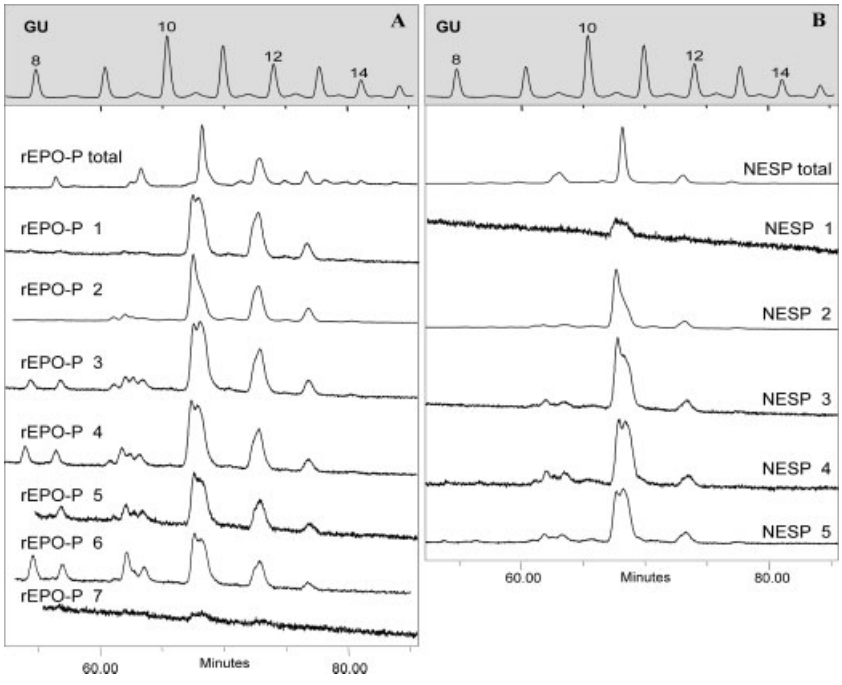

Figure 9. Normal-phase HPLC profiles of desialylated 2-AB-labeled *N*-glycans from 2-DE spots. (A) rEPO-P (1 for acidic, to 7 for basic spot). (B) NESP (1 for acidic, to 5 for basic spot). Profiles are standardized against dextran hydrolysate (GU) (upper panel in gray).

Mass spectrometric analysis allowed the structural identification of the glycans contained in the different spots. The mass spectrum of the most acidic spot (spot 1) showed almost exclusively tetra-antennary type structures containing 3–4 sialic acid residues and 1–2 LacNAc repeats. In the next spot, the intensity of these peaks changed in favor of the trisialo-components and already in the third spot biantennary glycans could be appreciated. In the following spots the intensity of tri- and biantennary structures increased whereas the tetra-antennary decreased. Finally, in spot 6 no

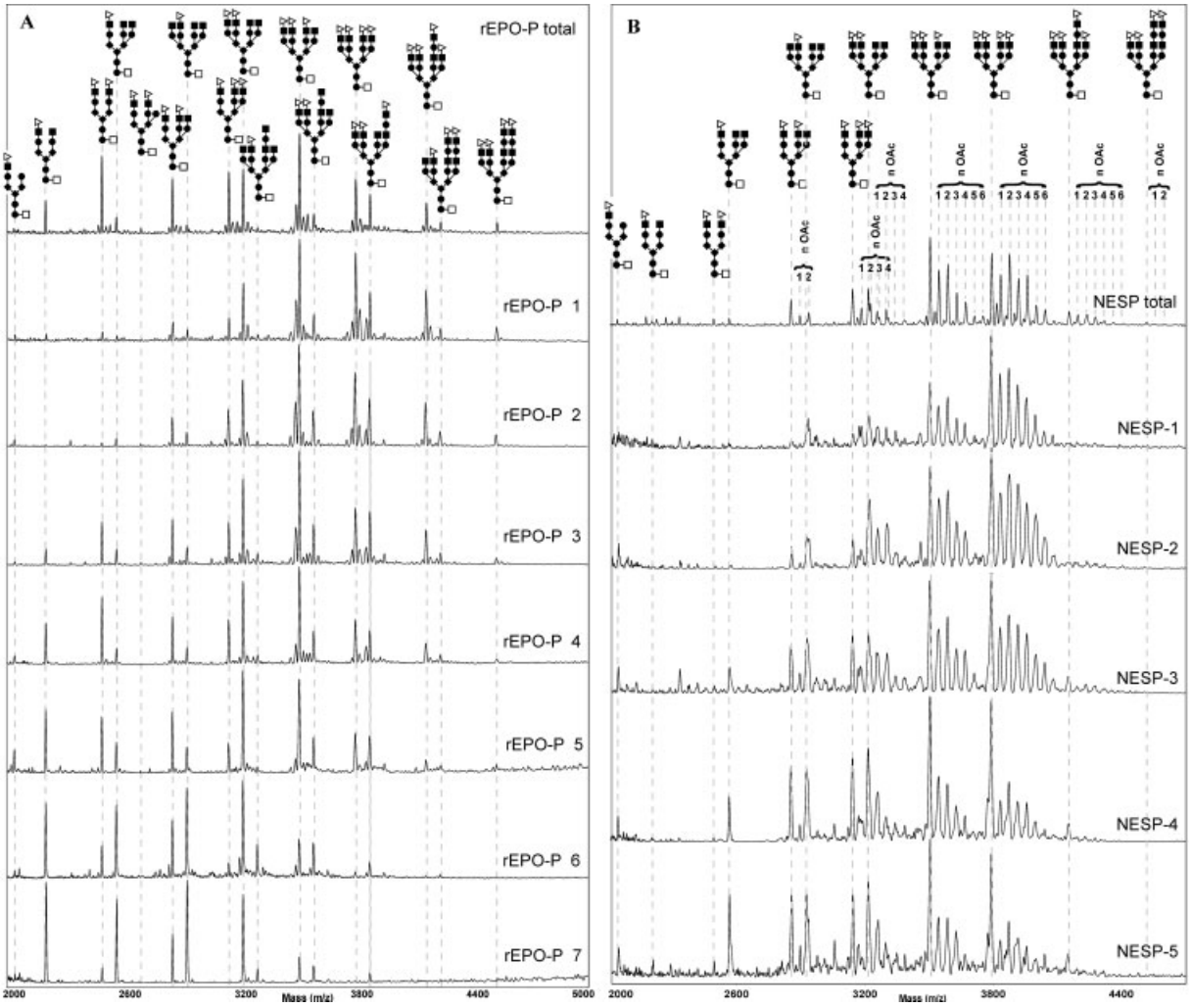

Figure 10. Negative-ion MALDI mass spectra of 2-AB-labeled *N*-glycans from 2-DE spots. (A) rEPO-P (1 for more acidic, to 7 for more basic spot). (B) NESP (1 for more acidic, to 5 for the more basic). Short-hand notation: (□) fucose, (●) *N*-acetylglucosamine, (◆) mannose, (■) galactose, (△) sialic acid. *n*OAc: O-acetylated sialic acids residues (where *n* = 0–7 indicate the number of substituents in a single *N*-glycan).

LacNAc-repeat containing structures were observed and monosialylated glycans accounted for the majority. Subsequently, mass spectra were integrated and each peak expressed as a relative percentage. Trend-lines were elaborated for the number of sialic acid residues *per* glycan in each spot and are visualized in Fig. 11. The most evident tendencies were observed for the least acidic spots (rEPO-7/6) in which tetrasialylated glycans were absent (rEPO-7) or account for less than ~1.2% (rEPO-6) while monosialylated glycans represented nearly 50% in both. The most acidic spots (rEPO-1/2) displayed the inverse trend, with apparent equivalence of tri- and tetrasialo components in rEPO-1, and a favorable ratio for trisialylated over tetrasialylated structures in rEPO-2. This trend is progressively more evident in rEPO-3 in which di- and trisialylated structures are equivalent, and in rEPO-4/5 in which disialylated glycans became the most abundant.

Mass spectra for NESP (Fig. 10) showed similar trends as observed in the HPLC chromatograms. After integration the trend lines for the individual spots are displayed in Fig. 11. Despite the fact that NESP contains two additional *N*-glycosylation sites (upto eight additional sialic acid residues) with respect to rEPO, the microheterogeneity observed was less. This can be explained by the fact that NESP contains a less biantennary structures (from 0% in NESP-1 to 2.8% in NESP-5). Thus, the intensity-decrease of tetra-antennary type structures, in parallel to the intensity-increase of biantennary type structures was very gradual. Surprisingly, the relative amounts of trisialo glycans in the distinct spots remained fairly constant (33 ± 2%) whereas the variation appeared to originate from the relative amounts of tetrasialylated glycans (from 22–54%). This was also reflected in the trend lines of the distinct antennae in each spot. With the decrease of tetra-

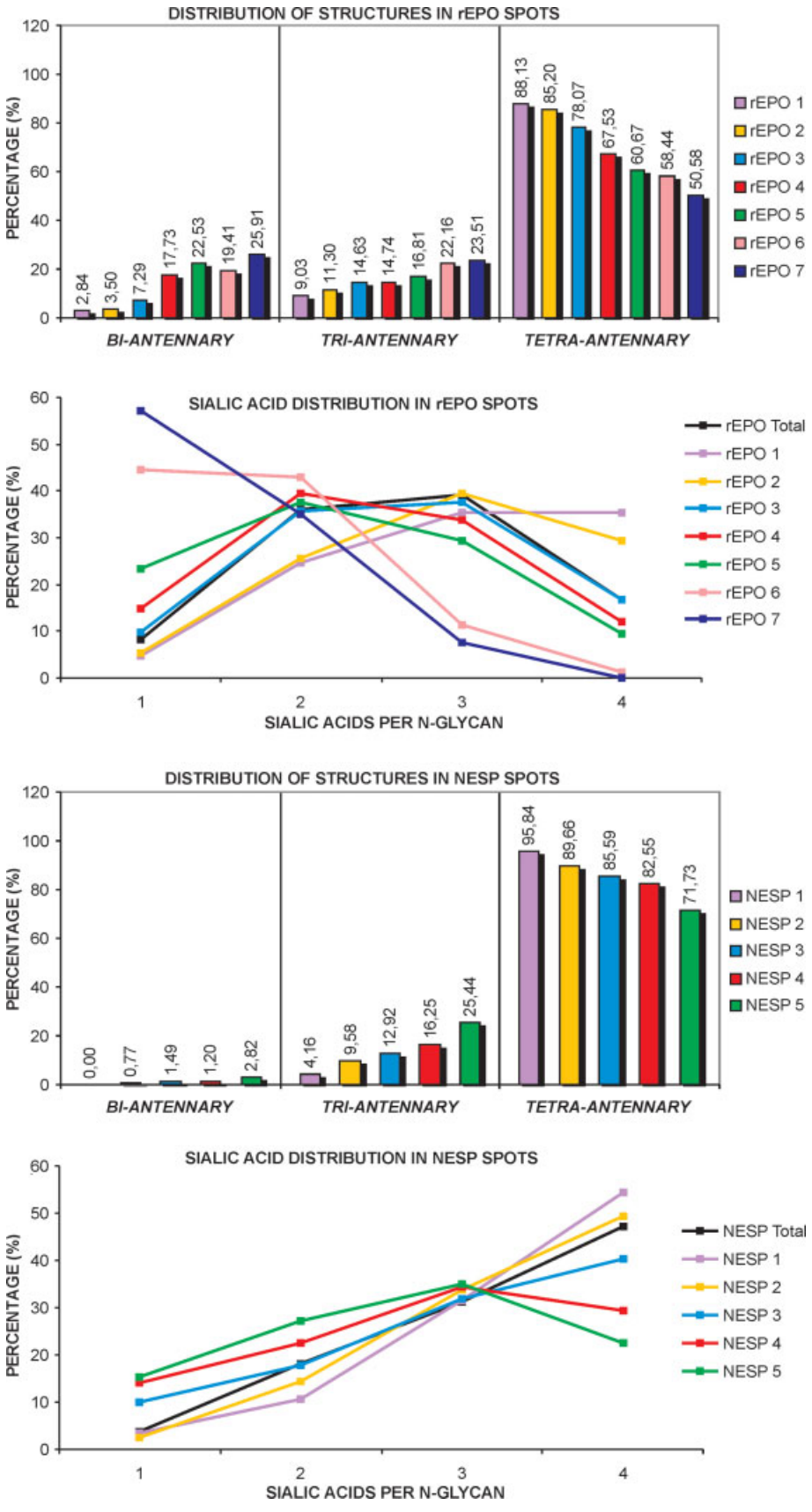

Figure 11. (A) Histogram showing relative percentage of bi-, tri-, and tetra-antennary *N*-glycans in each spot (tetra-antennary containing LacNAc repeats are included in tetra-antennary group). (A1) rEPO-P and (A2) NESP. (B) Trend-lines, based on mass spectra, indicating the number of sialic acids *per* glycan in each 2-DE spot. (B1) rEPO-P and (B2) NESP.

antennary structures (tetrasialylated) a clear increment in the amount of biantennary type glycans (disialylated) was observed, even though the latter only represent ~2% of all glycans present in NESP. Finally, the mass spectra showed no particular trend for the degree of *O*-acetylation; apparent maxima were observed for spots 2 and 3 whereas it appeared to decrease in spots 4 and 5.

4 Discussion

Strategies for the analysis of the proteome are necessarily evolving towards more specific protocols to address particular protein modifications [30]. In this context, the glycoproteome represents an extremely challenging endeavor due to the nontemplate driven mechanism of the phenomenon, the complexity of the structures and its tremendous impact on the physical (both p*I* and M_r) and biological properties of the protein [31]. In this paper, the standard proteomics approach 2-DE has been extended to cover the *N*-glycosylation in detail. Using two highly homologues glycoproteins (rEPO and NESP, 97% peptide homology and purified to have uniform sialic acid content), it is shown that subtle differences in glycosylation occur between adjacent spots [4], and how they influence the migration properties of a subset of glycoforms of a particular protein. In the development of the approach 2-DE was chosen over multidimensional chromatography as glycosylation is reflected as a characteristic "train" allowing identification. Furthermore, the conventional identification of the underlying protein is facilitated by removal of the sugars. It should be noted we could only observe seven isoforms for rEPO whereas eight have been described by the European Pharmacopea using CZE. It is evident that the diagonal appearance of such "train" is predominantly due to the differences in sialic acid content, and their impact on the hydrodynamic volume, of the glycoforms [13]. This is of particular interest in the case of recombinant erythropoietins, as their endogenous counterpart migrates in ~13 different spots, in between the p*I* values of rEPO and NESP, but does not show the diagonal tendency [28, 32]. Thus, one could deduce from the 2-DE analysis already that urinary erythropoietin (uEPO) should contain charges other than sialic acids. Recently, Belalcazar *et al*. [29] confirmed this using different enzymatic digestions of uEPO. In the analysis of the glycosylation contained in a single spot, enzymatic deglycosylation is mandatory to preserve the integrity of both the protein and the carbohydrate chains. At present, *N*-glycans can be released by endoglycanases but for *O*-glycans the one existing enzyme only addresses T-antigenic structures. In case preservation of the underlying protein is not mandatory chemical approaches including hydrazinolysis or alkaline release may be considered. After liberation from the protein scaffold, conservation *N*-glycans throughout all further steps in the analysis is of particular interest. The most vulnerable carbohydrate residue is sialic acid and throughout the different steps of the analytical procedure particular attention to this aspect was paid. As such, during the glycans extraction from the gel, ACN dehydration was preferred over sonication [33]. Another critical point is the derivatization procedure with 2-AB. This label was preferred over the more sensitive 2-aminobenzoic acid [34] as it does not introduce an additional charge (*i.e.*, polarity) to all glycans that complicates charge analysis by WAX and is more difficult to ionise in negative ion mode MS. The introduction of the fluorophore at the reducing-end sugar is carried out in a slightly acidic environment. Standard conditions described by Bigge *et al*. [20] claim that 2 h at 65°C yields an optimum between labeling and desialylation (only 2%). Nevertheless, Watanabe *et al*. [35] claimed a significant loss of sialic acids and proposed lowering the temperature to 37°C and prolonging the incubation to 16 h in order keep the labeling yield. In our hands, and employing a mixture of tetraantennary, multisialylated structures both protocols rendered similar labeling yields and structure preservation. Subsequent analyses by HPLC-FLD use buffers at pH 4.4. Special attention is required when fractions from a first separation (*i.e.*, charge analysis) are to be collected for further analysis by NP-HPLC or MALDI-TOF-MS as a loss of the label has been observed if the effluent is not neutralized immediately. Another point of care refers to the mass spectrometric analysis employing MALDI-TOF-MS because sialic acid residues may be lost during the crystallization, or during the actual ionization process. A comparison between different matrices (*e.g.*, DHB, sDHB, THAP, AZT [6]) that yield the best ionization for carbohydrates did not provide conclusive evidence in terms of signals (for different size or charge content) nor intensity to prioritize any for which DHB was employed. An important factor is the ionization energy employed during the analysis. An optimum between efficiency and degradation has to be found for each particular sample. In general, linear ion-mode offers best sensitivity in detriment of the resolution. Reflectron-mode (best resolution but lower sensitivity) offers yet another analytical detail that can be employed to minimize analyte degradation (*i.e.*, desialylation) during ionization. Postsource fragmentation (primarily desialylation in carbohydrates) occurs when the analyte has received a minimum of surplus energy that impedes its intact arrival at the detector. This is manifested as a broad peak ~+20 Da from the desialylated structure and clearly distinguishable from other well-resolved monoisotopic peaks. Decreasing the laser intensity to the point where metastable fragmentation products disappear, minimizes sample degradation [36]. Then changing the analysis mode from reflectron to linear greatly enhances the sensitivity with maximum guarantee of sialic acid preservation. Following these guidelines, the same sialic acid content was observed in the mass spectrometric analysis of intact NESP (analysis before and after chemical desialylation, and taking into account that the mean value of a single sialic acid in NESP should be 333 Da in stead of 291 Da due to the degree of *O*-acetylation), the analysis of the total

N-glycan pool (deglycoyslation in solution, and compensating with a mean of one sialic acid residue for the *O*-glycans) and in the mean of the *N*-glycans derived from the individual spots. It is of utmost importance to assure that minimal degradation occurs during sample processing as the degree or extent of glycosylation, and sialylation in particular, are associated with several glycan processing related pathologies such as CDG [37], rheumatoid arthritis, fetal alcohol syndrome, or carbohydrate-mediated biomolecular interactions (viral infections, cancer metastasis, *etc.*). With respect to carbohydrate-mediated interactions it is known that the recombinant pharmaceuticals employed here are engineered and purified for a high sialic acid content to prevent interactions with the hepatic galactosyl-receptor and thus clearance from circulation [38]. Another structural element that has been suggested to confer a prolonged half-life to glycoprotein drugs refers to the *O*-acetylation of the sialic acid residues [39]. In this respect the higher efficacy of NESP with respect to rEPO in circulation (administration once a week *vs.* three times *per* week, respectively) [7] could not only correspond to the additional *N*-glycans but also to the higher degree of *O*-acetylation contained in the former (0–7 *O*-acetyl groups *per N*-glycan for NESP and only 0–2 *O*-acetyl groups *per N*-glycan for rEPO) [40]. This structural element can be analyzed separately by the sialic acid analysis employing DMB [41] but is also easily picked up in the mass spectrometric analyses. Moreover, following sialidase digestion in RAAM, subsequent mass spectrometric analysis will enable unambiguous localization of the *O*-acetyl groups in the sialic acid, and the released sialic acid residues could ultimately be employed for DMB analysis to identify the substitution position. Overall, following the 2-DE separation the glycoproteomics strategy is composed of four main elements (WAX, NP, RAAM, and MS) that can be applied as a function of the degree of structural detail required. From the incorporation of a fluorescent group in a 1:1 stoichiometry an accurate quantification of charges (WAX) or individual glycans (NP) can be achieved. The GU value provides an indication of the structures present and a confirmation can be obtained through the targeted use of specific enzymes. Finally, MS allows both the corroboration of the chromatographic data as well as the determination of smaller structural elements. All together, the approach presented here is fully compatible with the current standard in proteomics analysis with the added value of addressing the most important PTM in a relatively rapid, straight-forward, and reliable manner. No doubt that this will contribute to a more comprehensive analysis in several research areas including clinical environments, drug quality control, study of specific cell-type glycosylation patterns [42], or even anti-doping control analysis.

The authors are thankful to Belen Cano Avalos for technical support. This work has been carried out with financial support from WADA.

5 References

[1] Kuster, B., Krogh, T. N., Mortz, E., Harvey, D. J., Glycosylation analysis of gel-separated proteins. *Proteomics* 2001, *1*, 350–361.

[2] Jenkins, N., Parekh, R. B., James, D. C., Getting the glycosylation right: Implications for the biotechnology industry. *Nat. Biotechnol.* 1996, *14*, 975–981.

[3] Mills, P. B., Mills, K., Johnson, A. W., Clayton, P. T. *et al.*, Analysis by matrix assisted laser desorption/ionisation-time of flight mass spectrometry of the post-translational modifications of alpha 1-antitrypsin isoforms separated by two-dimensional polyacrylamide gel electrophoresis. *Proteomics* 2001, *1*, 778–786.

[4] Zhou, Q., Park, S. H., Boucher, S., Higgins, E. *et al.*, N-linked oligosaccharide analysis of glycoprotein bands from isoelectric focusing gels. *Anal. Biochem.* 2004, *335*, 10–16.

[5] Rudd, P. M., Colominas, C., Royle, L., Murphy, N. *et al.*, A high-performance liquid chromatography based strategy for rapid, sensitive sequencing of N-linked oligosaccharide modifications to proteins in sodium dodecyl sulphate polyacrylamide electrophoresis gel bands. *Proteomics* 2001, *1*, 285–294.

[6] Harvey, D. J., Proteomic analysis of glycosylation: Structural determination of N- and O-linked glycans by mass spectrometry. *Expert. Rev. Proteomics*. 2005, *2*, 87–101.

[7] Egrie, J. C., Browne, J. K., Development and characterization of novel erythropoiesis stimulating protein (NESP). *Br. J. Cancer* 2001, *84*, 3–10.

[8] Schlags, W., Lachmann, B., Walther, M., Kratzel, M. *et al.*, Two-dimensional electrophoresis of recombinant human erythropoietin: A future method for the European Pharmacopoeia? *Proteomics* 2002, *2*, 679–682.

[9] Caldini, A., Moneti, G., Fanelli, A., Bruschettini, A. *et al.*, Epoetin alpha, epoetin beta and darbepoetin alfa: Two-dimensional gel electrophoresis isoforms characterization and mass spectrometry analysis. *Proteomics* 2003, *3*, 937–941.

[10] Restelli, V., Wang, M. D., Huzel, N., Ethier, M. *et al.*, The effect of dissolved oxygen on the production and the glycosylation profile of recombinant human erythropoietin produced from CHO cells. *Biotechnol. Bioeng.* 2006, *94*, 481–494.

[11] Wopereis, S., Grunewald, S., Huijben, K. M., Morava, E. *et al.*, Transferrin and apolipoprotein C-III isofocusing are complementary in the diagnosis of N- and O-glycan biosynthesis defects. *Clin. Chem.* 2007, *53*, 180–187.

[12] Kleinert, P., Kuster, T., Arnold, D., Jaeken, J. *et al.*, Effect of glycosylation on the protein pattern in 2-D-gel electrophoresis. *Proteomics* 2007, *7*, 15–22.

[13] He, Z., Aristoteli, L. P., Kritharides, L., Garner, B., HPLC analysis of discrete haptoglobin isoform N-linked oligosaccharides following 2D-PAGE isolation. *Biochem. Biophys. Res. Commun.* 2006, *343*, 496–503.

[14] Schellekens, H., Biosimilar epoetins: How similar are they? *Eur. J. Hosp. Pharm.* 2004, *3*, 43–47.

[15] Lasne, F., Martin, L., Crepin, N., de Ceaurriz, J., Detection of isoelectric profiles of erythropoietin in urine: Differentiation of natural and administered recombinant hormones. *Anal. Biochem.* 2002, *311*, 119–126.

[16] Lasne, F., Double-blotting: A solution to the problem of nonspecific binding of secondary antibodies in immunoblotting procedures. *J. Immunol. Methods* 2003, *276*, 223–226.

[17] Shevchenko, A., Wilm, M., Vorm, O., Mann, M., Mass spectrometric sequencing of proteins silver-stained polyacrylamide gels. *Anal. Chem.* 1996, *68*, 850–858.

[18] Stubiger, G., Marchetti, M., Nagano, M., Reichel, C. *et al.*, Characterisation of intact recombinant human erythropoietins applied in doping by means of planar gel electrophoretic techniques and matrix-assisted laser desorption/ionisation linear time-of-flight mass spectrometry. *Rapid Commun. Mass Spectrom.* 2005, *19*, 728–742.

[19] Packer, N. H., Lawson, M. A., Jardine, D. R., Redmond, J. W., A general approach to desalting oligosaccharides released from glycoproteins. *Glycoconj. J.* 1998, *15*, 737–747.

[20] Bigge, J. C., Patel, T. P., Bruce, J. A., Goulding, P. N. *et al.*, Nonselective and efficient fluorescent labeling of glycans using 2-amino benzamide and anthranilic acid. *Anal. Biochem.* 1995, *230*, 229–238.

[21] Gobom, J., Nordhoff, E., Mirgorodskaya, E., Ekman, R. *et al.*, Sample purification and preparation technique based on nano-scale reversed-phase columns for the sensitive analysis of complex peptide mixtures by matrix-assisted laser desorption/ionization mass spectrometry. *J. Mass Spectrom.* 1999, *34*, 105–116.

[22] Guile, G. R., Rudd, P. M., Wing, D. R., Prime, S. B. *et al.*, A rapid high-resolution high-performance liquid chromatographic method for separating glycan mixtures and analyzing oligosaccharide profiles. *Anal. Biochem.* 1996, *240*, 210–226.

[23] Royle, L., Radcliffe, C. M., Dwek, R. A., Rudd, P. M., Detailed structural analysis of N-glycans released from glycoproteins in SDS-PAGE gel bands using HPLC combined with exoglycosidase array digestions. *Methods Mol. Biol.* 2006, *347*, 125–143.

[24] Stubiger, G., Marchetti, M., Nagano, M., Grimm, R. *et al.*, Characterization of N- and O-glycopeptides of recombinant human erythropoietins as potential biomarkers for doping analysis by means of microscale sample purification combined with MALDI-TOF and quadrupole IT/RTOF mass spectrometry. *J. Sep. Sci.* 2005, *28*, 1764–1778.

[25] Royle, L., Roos, A., Harvey, D. J., Wormald, M. R. *et al.*, Secretory IgA N- and O-glycans provide a link between the innate and adaptive immune systems. *J. Biol. Chem.* 2003, *278*, 20140–20153.

[26] Hokke, C. H., Bergwerff, A. A., van Dedem, G. W., Kamerling, J. P. *et al.*, Structural analysis of the sialylated N- and O-linked carbohydrate chains of recombinant human erythropoietin expressed in Chinese hamster ovary cells. Sialylation patterns and branch location of dimeric N-acetyllactosamine units. *Eur. J. Biochem.* 1995, *228*, 981–1008.

[27] Neususs, C., Demelbauer, U., Pelzing, M., Glycoform characterization of intact erythropoietin by capillary electrophoresis-electrospray-time of flight-mass spectrometry. *Electrophoresis* 2005, *26*, 1442–1450.

[28] Skibeli, V., Nissen-Lie, G., Torjesen, P., Sugar profiling proves that human serum erythropoietin differs from recombinant human erythropoietin. *Blood* 2001, *98*, 3626–3634.

[29] Belalcazar, V., Gutiérrez Gallego, R., Llop, E., Segura, J. *et al.*, Assessing the instability of the isoelectric focusing patterns of erythropoietin in urine. *Electrophoresis* 2006, *27*, 4387–4395.

[30] Carr, S. A., Annan, R. S., Huddleston, M. J., Mapping post-translational modifications of proteins by MS-based selective detection: Application to phosphoproteomics. *Methods Enzymol.* 2005, *405*, 82–115.

[31] Geyer, H., Geyer, R., Strategies for analysis of glycoprotein glycosylation. *Biochim. Biophys. Acta* 2006, *1764*, 1853–1869.

[32] Khan, A., Grinyer, J., Truong, S. T., Breen, E. J. *et al.*, New urinary EPO drug testing method using two-dimensional gel electrophoresis. *Clin. Chim. Acta* 2005, *358*, 119–130.

[33] Kuster, B., Wheeler, S. F., Hunter, A. P., Dwek, R. A. *et al.*, Sequencing of N-linked oligosaccharides directly from protein gels: In-gel deglycosylation followed by matrix-assisted laser desorption/ionization mass spectrometry and normal-phase high-performance liquid chromatography. *Anal. Biochem.* 1997, *250*, 82–101.

[34] Anumula, K. R., Advances in fluorescence derivatization methods for high-performance liquid chromatographic analysis of glycoprotein carbohydrates. *Anal. Biochem.* 2006, *350*, 1–23.

[35] Watanabe, T., Inoue, N., Kutsukake, T., Matsuki, S. *et al.*, Labeling conditions using a 2-aminobenzamide reagent for quantitative analysis of sialo-oligosaccharides. *Biol. Pharm. Bull.* 2000, *23*, 269–273.

[36] Sanz-Nebot, V., Benavente, F., Gimenez, E., Barbosa, J., Capillary electrophoresis and matrix-assisted laser desorption/ionization-time of flight-mass spectrometry for analysis of the novel erythropoiesis-stimulating protein (NESP). *Electrophoresis* 2005, *26*, 1451–1456.

[37] Sagi, D., Kienz, P., Denecke, J., Marquardt, T. *et al.*, Glycoproteomics of N-glycosylation by in-gel deglycosylation and matrix-assisted laser desorption/ionisation-time of flight mass spectrometry mapping: Application to congenital disorders of glycosylation. *Proteomics*. 2005, *5*, 2689–2701.

[38] Yuen, C. T., Storring, P. L., Tiplady, R. J., Izquierdo, M. *et al.*, Relationships between the N-glycan structures and biological activities of recombinant human erythropoietins produced using different culture conditions and purification procedures. *Br. J. Haematol.* 2003, *121*, 511–526.

[39] Corfield, T., Bacterial sialidases – roles in pathogenicity and nutrition. *Glycobiology* 1992, *2*, 509–521.

[40] Rush, R. S., Derby, P. L., Smith, D. M., Merry, C. *et al.*, Microheterogeneity of erythropoietin carbohydrate structure. *Anal. Chem.* 1995, *67*, 1442–1452.

[41] Hokke, C. H., Bergwerff, A. A., van Dedem, G. W., van Oostrum, J. *et al.*, Sialylated carbohydrate chains of recombinant human glycoproteins expressed in Chinese hamster ovary cells contain traces of N-glycolylneuraminic acid. *FEBS Lett.* 1990, *275*, 9–14.

[42] Toledo, J. R., Sanchez, O., Montesino, S. R., Fernandez, G. Y. *et al.*, Differential in vitro and in vivo glycosylation of human erythropoietin expressed in adenovirally transduced mouse mammary epithelial cells. *Biochim. Biophys. Acta* 2005, *1726*, 48–56.

